GEOLOGICAL SURVEY OF CANADA
OPEN FILE 7319

Petrographic and cathodoluminescence characterization of apatite from the Sue-Dianne and Brooke IOCG mineralization systems, Great Bear magmatic zone, Northwest Territories

P. Lypaczewski, P.X. Normandeau, J. Paquette, and I. McMartin

2013

Natural Resources Canada
Ressources naturelles Canada

GEOLOGICAL SURVEY OF CANADA
OPEN FILE 7319

Petrographic and cathodoluminescence characterization of apatite from the Sue-Dianne and Brooke IOCG mineralization systems, Great Bear magmatic zone, Northwest Territories

P. Lypaczewski[1], P.X. Normandeau[1], J. Paquette[1], and I. McMartin[2]

[1] Department of Earth and Planetary Sciences, McGill University, Montreal, QC H3A 0E8
[2] Geological Survey of Canada, 601 Booth St., Ottawa, ON K1A 0E8

2013

©Her Majesty the Queen in Right of Canada 2013

doi: 10.4095/292369

This publication is available for free download through GEOSCAN (http://geoscan.ess.nrcan.gc.ca).

Recommended citation
Lypaczewski, P., Normandeau, P.X., Paquette, J., and McMartin, I., 2013. Petrographic and cathodoluminescence characterization of apatite from the Sue-Dianne and Brooke IOCG mineralization systems, Great Bear magmatic zone, Northwest Territories; Geological Survey of Canada, Open File 7319. doi: 10.4095/292369

Publications in this series have not been edited; they are released as submitted by the author.

TABLE OF CONTENTS

Abstract ………………………………………………………………………………… p. 1
Introduction ……………………………………………………………………………. p. 1
Methodology …………………………………………………………………………… p. 2
    Sample selection ………………………………………………………………….. p. 2
    Transmitted-light microscopy …………………………………………………….. p. 5
    Cathodoluminescence microscopy ……………………………………………….. p. 5
    Scanning electron microscopy …………………………………………………… p. 6
Results ....…………………………………………………………………………….. p. 6
    Petrography ………………………………………………………………………. p. 7
    Cathodoluminescence …………………………………………………………… p. 8
    Apatite occurrence ……………………………………………………………….. p. 12
Discussion .... p. 12
Suggestions for future work ....……………………………………………… p. 13
Acknowledgements ……………………………………………………………………… p. 13
References ………………………………………………………………………….…...... p. 14

Appendices

A. Photomicrographs of thin sections in PPL and CL modes
B. Backscatter electron and EDX images on apatite crystals
C. Detailed observations of thin sections

LIST OF TABLES

1. Summary of sample locations and alteration types ....…………………………… p. 4
2. Summary of petrographic and cathodoluminescence observations........................... p. 10-11

LIST OF FIGURES

1. Location map of IOCG systems within the Great Bear magmatic zone .... p. 2
2. Regional bedrock geology of the Sue-Dianne deposit and Brooke Zone area with sample locations .... p. 2
3. Regional bedrock geology of the Fab Lake system area. Sample site locations are shown.. p. 5
4. CL photomicrographs of A) scheelite crystal (bright blue) in feldspar matrix (faint blue) with micron-sized apatite (green specs) and B) calcite (orange) and apatite (green).. p. 8
5. Apatite grain where darker zones (in BSE) correspond to brighter CL, and inversely. From backscatter electron image 09CQA0026C01_06. BSE; the red square shows the same grain in CL. White dots are mineral inclusions, possibly monazite.................. p. 9
6. Same apatite crystal imaged in BSE (SEM, left) and CL (right) showing that the blue CL color matches the brighter (heavier element-enriched) zones where REEs are detected by EDX.. p. 9

PETROGRAPHIC AND CATHODOLUMINESCENCE CHARACTERIZATION OF APATITE FROM THE SUE-DIANNE AND BROOKE IOCG MINERALIZATION SYSTEMS, GREAT BEAR MAGMATIC ZONE, NORTHWEST TERRITORIES

P. Lypaczewski[1], P.X. Normandeau[1], J. Paquette[1], and I. McMartin[2]

1 Department of Earth and Planetary Sciences, McGill University, Montreal, QC H3A 0E8

2 Geological Survey of Canada, 601 Booth St., Ottawa, ON K1A 0E8

ABSTRACT

Apatite is the main REE-bearing phase in 19 thin sections from two mineralized systems and their host rocks, the Cu-Ag-(Au) Sue-Dianne IOCG deposit and the nearby Brooke Zone, located within the southern Great Bear magmatic zone, Northwest Territories, Canada. The thin sections show a range of IOCG-related alterations and igneous protoliths. Apatite occurs in all thin sections, in amounts ranging between traces to 5-10%. It can be divided into four populations on the basis of size, cathodoluminescence (CL) response and petrographic association: 1) small euhedral apatite (20-40 µm), occurring in clusters of 5 to 20 grains, generally free of inclusions, found in the volcaniclastic samples; 2) single apatite crystals (60-80 µm) with pitted edges, numerous fluid inclusions and sometimes monazite and hematite inclusions; 3) large single apatite crystals (100-300 µm) within epidote veins, sometimes associated with scheelite; and 4) large fractured apatite crystals (0.5 to 4 mm) with heavy hematite staining associated with hydrothermal breccias. The first 3 populations have a green to yellow CL response and the third population shows some irregular zoning. The fourth population shows a blue CL tint, with irregular green zones throughout grains or near the crystal rims. In that fourth population, mineral inclusions with an orange CL response are likely calcite. Group 3 and 4 also show an heterogeneous REE distribution within crystals under EDX. Given the overprinting of multiple alteration types in many of the specimens, additional work is needed to relate these apatite populations to specific alteration stages associated with IOCG-type mineralization. However, the presence of apatite coarse enough to be picked from glacial sediment samples and showing distinctive CL signatures in rocks related to IOCG mineralization suggests potential as an indicator mineral method.

INTRODUCTION

While apatite has potential to be a good indicator mineral in iron oxide copper-gold (IOCG) Kiruna-type deposits where it is a major mineral of the ore zone (Bonyadi, 2011), it is also present as an accessory mineral throughout the IOCG spectrum. It has been found to be a good resistate mineral in both weathered and glaciated terrains (De Toledo et al., 2004; Bouzari et al., 2011). For example, apatite is commonly present in till from the Great Bear magmatic zone (Gbmz) in amounts ranging between traces to 20% of the heavy mineral fraction (0.25-0.5 mm, separated at SG>3.2) with values above 2% found over or down-ice from IOCG systems (Normandeau et al., 2011). It has the ability to record geochemical conditions during its formation or subsequent alteration (Harlov et al., 2002; Harlov et al., 2005; Bouzari et al., 2011). Rare earth elements (REEs), as well as Sr^{2+}, Fe^{2+} and Mn^{2+}, can be incorporated in apatite's Ca^{2+} sites, usually related to the $Ca^{2+} + P^{5+} \rightarrow REE^{3+} + Si^{4+}$ coupled substitution (Coulson and Chambers, 1996). The variations in Mn, Fe and REEs concentrations impart different colors to apatite in cathodoluminescence (CL) (Kempe & Gotze, 2002) allowing a preliminary assessment of compositional variation between and within grains. Apatite can also incorporate chalcophile elements, allowing the recognition of grains derived from mineralized zones (Belousova et al., 2002).

An undergraduate research project from McGill University, in partnership with the Geo-mapping for Energy and Minerals (GEM) IOCG Great Bear Project at the Geological Survey of Canada, was undertaken to identify and characterize the morphology and habits of the apatite and other REE-bearing phases present in the magnetite to hematite group Cu-Ag-(Au) IOCG Sue Dianne deposit (Mumin et al. 2010) and the nearby Brooke Zone and their host rock lithologies, located in the southern Great Bear magmatic zone, Northwest Territories, Canada (Figure 1). The results of this work will assist an ongoing doctoral research project by Philippe X. Normandeau at McGill University, which aims to develop a drift prospecting approach to IOCG exploration in glaciated terrain. This study was accomplished using transmitted light and cathodoluminescence optical petrography, together with backscatter electron imaging and energy dispersive x-ray spectroscopy analysis from a scanning electron microscope on a selection of bedrock thin sections.

METHODOLOGY

Sample selection

Samples from outcrops near and within the Sue-Dianne and Brooke IOCG mineralization systems (Figure 2) were selected from a suite of samples collected as part of the GEM IOCG Great Bear project in 2009 and 2010. The samples consisted of 14 polished thin sections accompanied by field descriptions of the sampled units. Table 1 provides the sample locations. These samples were selected to represent a range of IOCG alterations (Table 2) within the various lithologies exposed near the two mineralized complexes (Corriveau et al., 2010). Sue-Dianne mineralization surface samples (09CQA1009A1, 09CA1009B1) are from the hematite-dominated iron-oxides zone (Camier, 2002; Mumin et al., 2010), and a drill core sample from the magnetite-dominated zone, provided by Fortune Mineral Lt. (2507A), was added to the selection to better represent the Sue-Dianne mineralization.

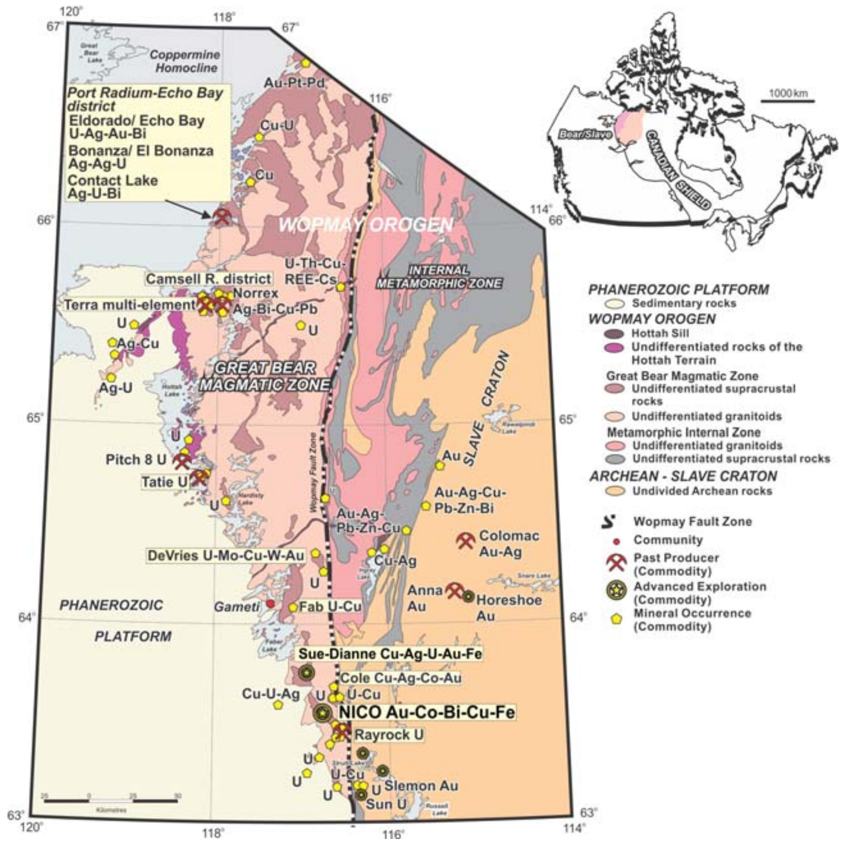

Figure 1. The Great Bear magmatic zone bedrock geology, mineral occurrences and past-producing mines (modified from Corriveau et al. 2012). The Sue-Dianne deposit (and nearby Brooke Zone) is located in the southern part of the GBmz. Inset map locates the Wopmay orogen (Bear Province) and adjacent Slave craton at the western edge of the Canadian Shield.

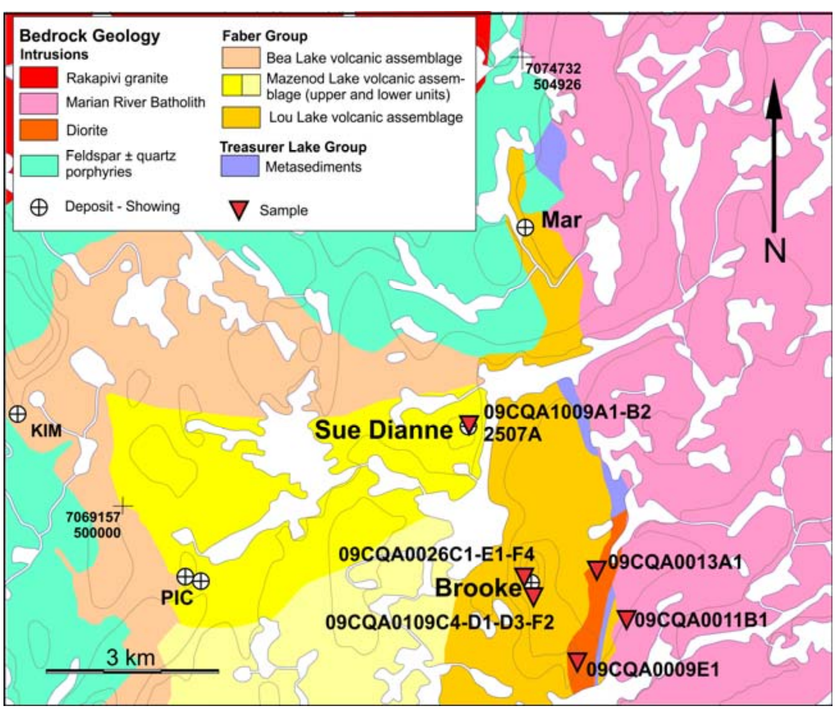

Figure 2. Regional bedrock geology of the Sue-Dianne deposit and Brooke Zone area (from Camier, 2002). Sample site locations are shown.

Table 1. Summary of sample locations

Sample	Location	Easting	Northing
09CQA0009E01	Regional	505634.13	7067394.2
09CQA0011B01	Regional	506131.74	7067868.88
09CQA0013A01	Regional	505887.35	7068580.82
09CQA0026C01	Brooke zone	505005.7	7068450.41
09CQA0026E01	Brooke zone	505005.7	7068450.41
09CQA0026F04	Brooke zone	505005.7	7068450.41
09CQA0109D01	Brooke zone	505043.31	7068270.64
09CQA0109F02	Brooke zone	505043.31	7068270.64
09CQA0109D03	Brooke zone	505043.31	7068270.64
09CQA0109C04	Brooke zone	505043.31	7068270.64
09CQA0026E04-1	Brooke zone	505005.7	7068450.41
09CQA0026E04-2	Brooke zone	505005.7	7068450.41
09CQA1009A1	Sue Dianne	504266.07	7070311.31
09CQA1009B1	Sue Dianne	504266.07	7070311.31
2507A	Sue Dianne, core	5042XX	70703XX
11PUA086B04	Fab	493377.67	7114864.21
11PUA538D01	Fab	492742.27	7115753.78
11PUA538C01	Fab	492742.27	7115753.78
11PUA084C01	Fab	494180.61	7110513.47

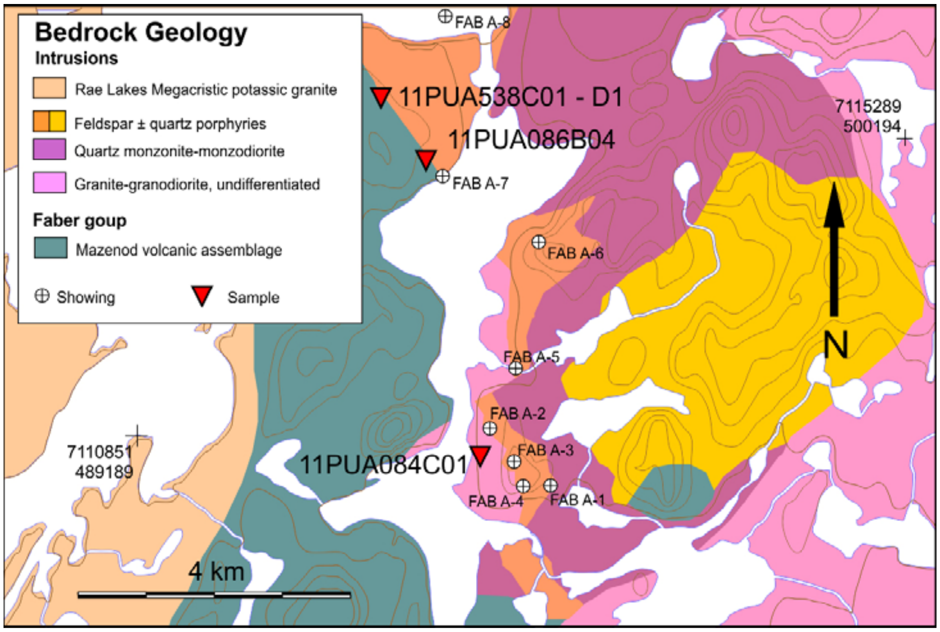

Figure3. Regional bedrock geology of the Fab Lake system area (from Gandhi et al., 2001). Sample site locations are shown.

Four additional polished thin sections from a third magnetite-group IOCG system (Fab) became available at the end of this study (Fig. 3; see Fig. 1 for location of Fab system) (Potter et al., 2012). As they provided a valuable contribution to the apatite characterization in IOCG settings from the GBmz, their preliminary description was added to this report. It is to be noted however that these last samples are derived from large, thorium-rich, amphibole veins within the Fab IOCG system. Therefore, the samples collected offer a valid representation of the Ca-Fe (HT) alteration of the Fab Lake system, mostly absent at surface in the Sue Dianne system.

Transmitted-light microscopy

Petrographic descriptions using transmitted-light microscopy were completed on each thin section sample using a Leica Model DME polarized microscope. Apatite grains were observed using the 50x objective and 10x ocular, and could only be observed in plane polarized light, as crossed polars made the low birefringence apatite indistinguishable from the surrounding microcrystalline silicates (e.g. feldspar, quartz).

Cathodoluminescence microscopy

Each thin section was examined using cathodoluminescence (CL) optical microscopy. Photomicrographs were taken in both transmitted plane polarized light (PPL) and optical CL mode and are provided in Appendix A. Exposure times and settings are included in the file name of each image, according to the format [ThinSectionNumber_PictureNumber – Voltage, Current, Exposure time, Gain]. As such, the filename '*09CQA0109C04_02 - 4.0kV, 0.5 mA, 6.9 s gain 5.0*' refers to the second photograph of thin section 09CQA0109C04, taken in CL mode with a beam set a 4kV and 0.5 mA, a camera exposure time of 6.9 seconds and a gain of 5.

The optimal combination of settings was found to be a 4.0 kV beam with an exposure time of 3-4 seconds, and a low gain of 5. Most importantly, a well adjusted electron beam focus was required. The optimal focus was found to be about 3 mm wide; a wider beam resulted in an intensity of CL emissions too low to allow a practical exposure time for the photography (under 15 seconds). When scanning through the thin section to locate an area of interest, the gain was adjusted to 25 and exposure times reduced to 250 - 400 milliseconds, allowing for an acceptable refreshing rate of the image. These settings, however, are only good for the initial observation of the samples in CL, due to luminescence aging. Murray and Oreskes (1997) analyzed the variation in CL response with exposure time, and found that the peaks at different wavelengths, produced by specific elements, exponentially decrease in intensity with exposure time, at different rates. In fact, a decrease in intensity by an average of 33% was noted over the first 8 minutes of exposure, often leading to change in the tint of the emission. This effect limits the usefulness of CL in determining the paragenesis of samples, since zoning in apatite grains of metasomatic or magmatic origin shows only faint contrast in CL and is strongly affected by luminescence aging.

Scanning electron microscopy

Petrographic descriptions and CL analysis were used to discriminate populations of apatite according to their morphology, CL response and petrographic association. A selection of representative grains from each population was then observed by backscatter electron imaging using a scanning electron microscope. Backscatter electron images (BSE) were taken using the Hitachi S-3000N variable pressure scanning electron microscope (SEM) at the Facility for Electron Microscopy Research (FEMR) at McGill University. The beam was set at 25 kV in variable pressure mode (set at 20 Pa). Single-point, non-quantitative compositional data was obtained using energy dispersive X-ray spectroscopy analysis (EDX) with the INCA analysis software. Readings were averaged over a live time period of 50 seconds and taken at multiple locations on and around apatite crystals. BSE and EDX data are provided in Appendix B.

RESULTS

Detailed petrographic observations of each thin section, together with a selection of SEM photomicrographs in PPL, CL and backscatter modes, are provided in Appendix C and summarized in Table 2. Alteration types provided in Table 2 are based on field observations, portable gamma-ray spectrometer data and bulk geochemistry analysis (Corriveau et al. 2010), while the mineral replacements are those observed in the sample and are most often the result of the late stage lower temperature alterations.

Petrography

09CQA0011B01, 09CQA0009E01: These samples are from the Marian River Batholith bordering the Sue Dianne and Brooke system to the east. 09CQA11B01 is part of the least altered granitic country rock while 09CQA0009E01 is cut within a quartz-feldspars-hematite hydrothermal vein.

09CQA0109F02, **09CQA0013A01:** These two samples are mostly altered to epidote and show evidence of previous alteration phases. The epidotisation is associated with magnetite in 09CQA0109F02 and Mg-rich chlorite in 09CQA0013A01. The alteration phases overprinted were not identified.

09CQA0026 series, 09CQA0109D01, 09CQA0109D03, 09CQA0109C04: Many samples consist of hematite-stained tuffs that show mineral replacement of intermediate intensity. Sample 09CQA0026F04 is one of the least replaced of these samples, with potassic feldspar clasts showing only a minor alteration to clay-size material. Other samples show a low amount of clay minerals, numerous monocrystalline clasts and a late microcrystalline silica matrix, all of them being overprinted by heavy hematite staining. 09CQA0109C04 also shows some minor late epidote alteration. In the samples showing more intense mineral replacements, such as 09CQA0026E04, the feldspar clasts are hardly identifiable, and the matrix is fairly homogeneous.

2507A, 09CQA1009A1, 09CQA1009B1: Mineralized samples from the Sue-Dianne deposit are brecciated and show intense replacements. The original mineral assemblages have been completely replaced by iron oxide, clays, chlorite, apatite and a microcrystalline silica matrix.

11PUA086B04, 11PUA538D01, 11PUA538C01, 11PUA084C01: All samples from the Fab Lake system are taken from a large amphibole rich vein. 11PUA086B04 is a coarse grained (>3 mm) assemblage of euhedral amphibole, muscovite and apatite with abundant hematite staining. 11PUA538D01 and 11PUA084C01 are composed of finer grained muscovite and amphibole, with rare apatite and traces of chlorite and clay replacements. 11PUA538C01 is an assemblage of coarse (>5 mm) potassic feldspar, plagioclase and quartz, locally altered to fine grained silica at crystal boundaries. Some potassic feldspar show incipient alteration to clay minerals. Biotite and chlorite are present. All are noteworthy for their more complexly zoned apatite than the samples from the Sue Dianne and Brooke system.

In all cases but for the two samples with major epidote alteration (09CQA0109F02 and 09CQA0013A01), the intensity of replacement generally correlates with the amount of iron oxide present, either in the form of a light hematite staining or a large amount of crystalline magnetite and/or hematite aggregates.

Cathodoluminescence (CL)

In CL, the luminescent phases were found to be apatite, scheelite, calcite with or without the background response of an altered feldspar and/or quartz matrix (Fig. 4). Calcite emits a characteristic red-orange color and cannot be mistaken for any other mineral specie. Feldspars emit the typical, faint, light blue response. Scheelite has a light blue color similar to that of feldspars but is far brighter. Apatite shows the most variation; it emits a greenish-yellow CL color in the majority of the samples, and a light lilac-blue to green color in the Sue-Dianne and Brooke mineralized samples and in the samples from the Fab Lake IOCG system.

CL zoning is present in most apatite grains but is patchy and irregular, with the exception of a few crystals also showing euhedral concentric zoning (09CQA0109C04, 2507A). Similar zoning patterns have been interpreted as the result of metasomatic alteration by Rae et al. (1996). The bright and darker zones in CL highlighting the observed patterns are also visible in the BSE images (Fig. 5), where brighter zones in CL correspond to darker zones in BSE mode. Kempe and Götze (2002) noted that decreased CL intensity in the core of apatite correlated with an increased quantity of Mn^{2+}, possibly indicating self-quenching at concentrations above 2.0 wt% Mn. These authors observed that the darker zones in CL might be due to increased relative concentrations of weakly responding REEs over strongly responding REEs rather than to a higher concentration of Mn^{2+}. Rae et al. (1996) reported that apatite derived from samples in close proximity to the hydrothermal fluids source had a more contrasting and complex zonation pattern than the ones coming from samples further away from it.

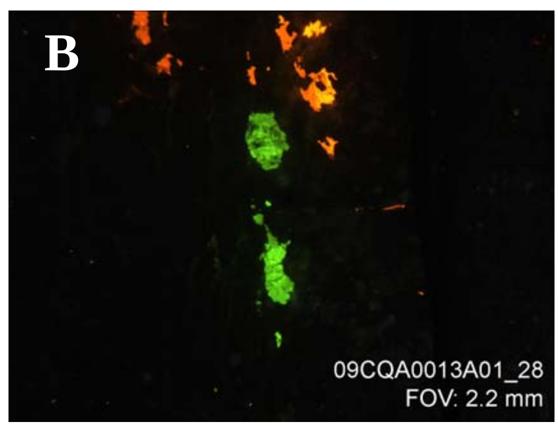

Figure 4. CL photomicrographs of: A) scheelite crystals (bright blue) in feldspar matrix (faint blue) with micron-sized apatite (green specs); B) calcite (orange) and apatite (green).

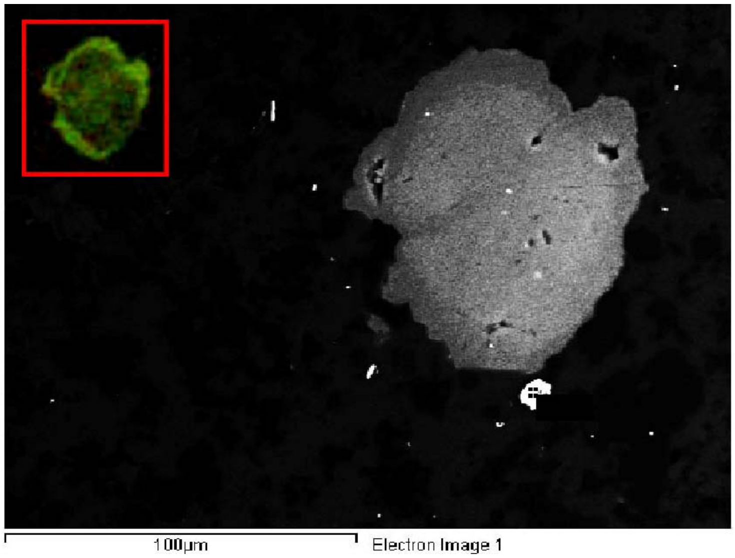

Figure 5. Apatite grain where darker zones (in BSE) correspond to brighter CL, and inversely. From backscatter electron image 09CQA0026C01_06. BSE; the red square shows the same grain in CL. White dots are mineral inclusions, possibly monazite.

The blue (CL) apatite from the brecciated mineralized zone at Sue-Dianne (09CQA1009A01, 09CQA1009B01, 2507A) shows hematite staining and brecciation during or after its crystallization. The main blue color is replaced by a green color often on the outer edges of the crystals and also along fractures in the apatite or in the form of stringers (09CQA0109C04, 11UPA086B04, 2507A). The green color is likely due to substitution of Ca^{2+} by Mn^{2+}, and the lilac-blue color to substitution of Ca^{2+} by REEs (Kempe & Gotze, 2002). This is supported by the BSE images, where blue zones are of lighter shades (2507A) (Fig. 6). These zones often show the presence of REEs in quantities above the EDX detection limit. The green zones in CL are darker in BSE images and do not show detectable REEs by EDX analysis.

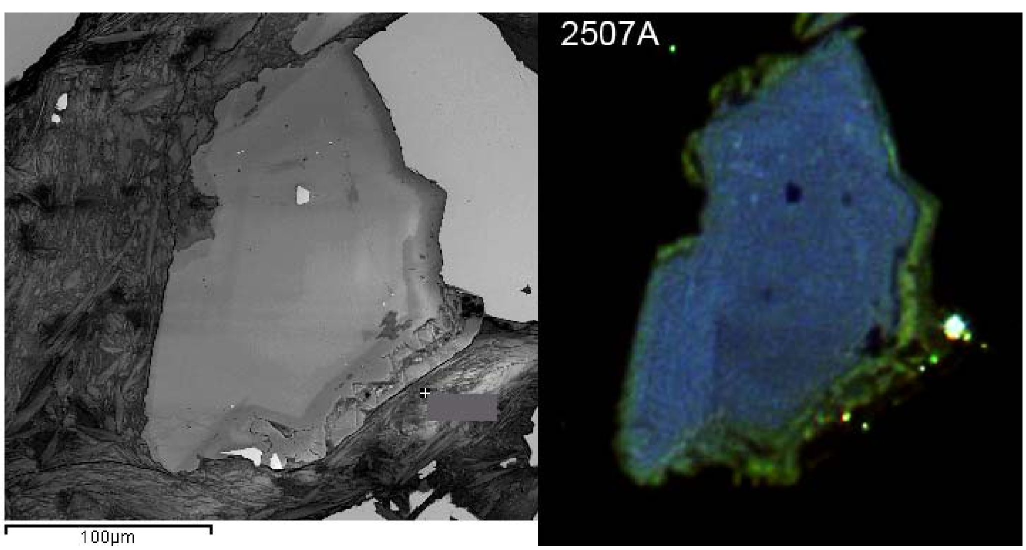

Figure 6. Same apatite crystal imaged in BSE (SEM, left) and CL (right) showing that the blue CL color matches the brighter (heavier element-enriched) zones where REEs are detected by EDX.

Table 2. Summary of petrographic and cathodoluminescence observations

ID	Alteration	Mineral replacement	Veins	Apatite location/Association	Apatite size	CL, additional information
09CQA0009E01	Qtz-Hem vein	Chl, Fe. K-spar overgrowth	None	In altered assemblages.	< 30 µm	Rare green-yellow point seen in CL, cannot be seen in PPL
09CQA0011B01	K alteration	Bt, amp -> chl. Plag -> Fe, Clay	Rare; Ep	- Common in chl	60-80 µm	Green-yellow, heterogeneous zonations, euhedral, numerous in chlorite.
				- Rare in feldspars	< 60 µm	
09CQA0013A01	Na-Ca-Fe (HT)	Ep, Si, K, Chl	Common; Ep, Chl	Disseminated in matrix	< 40 µm	Green-yellow, texture visible on larger grains. Numerous red (CL) calcite.
				At vein edges	80-200 µm	
09CQA0109F02	K, K-Fe (HT) ,K-Fe (LT), Ca-Fe (LT) alteration	Clay ± Si (early), Ep, Mag, Minor Pyrite	Numerous; Si (early). Ep ± Mag (Late)	- Early aggregate	40-80 µm	Green-yellow, in veins, homogeneous. Light blue (Intense); scheelite
				- In Ep. Veins	100-300 µm	
09CQA0109C04	K alteration	µm Si, Fe, Clay.	Common, Ep ± Ccp(Py?). Hem, Ep, Si, Clay.	In relict mafic crystals	30-60 µm, 100-180 µm	Grayish-blue-green, green-yellow, commonly show bright rim and zonations.
09CQA0026F04	K±Fe (HT) alteration	µm Si, Fe, Clay.	Few; Mag, Si.	Aggregates	80-120 µm	Green-yellow, heterogeneous zonations.
				Near old veinlets.	60-100 µm	
09CQA0026C01	Fe (HT), K alteration	µm Si, Fe, Clay	Rare; Ep	Dissiminated	50-100µm,	Green-yellow, heterogenous zonations, bright rim; metasomatic alteration.
09CQA0026E01		µm Si, Fe, Clay	Common; Hb, Chl, Mag, Qz.	- Aggregates.	20-40 µm	Green-yellow, heterogeneous zonations. Brownish patch in CL surrounding apatite aggregates.
				- Dissiminated	70-80 µm	
				- Near/in veins.	80-120 µm	
09CQA0109D01	K-Fe (HT to LT) alteration, brecciation	µm Si, Fe, Clay, Minor Ep	Early Si. Breccia; Mag ± Si	- In relict veinlets	70-90 µm	Green-yellow, faint heterogeneous zonations. Striated apatites. Relict mafic (?) zones appear brown in CL.
				- Less often In relict mafic zones	<40 µm	
09CQA0109D03	Fe±K (HT to LT) alteration, brecciation	µm Si, Fe, Clay, Minor Ep	Early Si. Breccia; Mag ± Si	In relict mafic zones	< 40 µm -80 µm	Green-yellow, heterogeneous, bright rim. Striated apatites. Relict mafic (?) zones easily seen in CL.
09CQA0026E04-1	Na (HT), K-Fe (HT) alteration, brecciation	µm Si, Clay, Ep ±Fe	Common; deformed, Py, Ep, Si.	Aggregates	20-30 µm	Green-yellow, minor het. zonations. Numerous blue scheelite.
				Dissiminated	60-80 µm	
09CQA0026E04-2	Na (HT), Fe (HT) alteration, brecciation	µm Si, Fe, Ep ±Clay	Numerous; deformed. Ep, Si, Chl, Mag	Aggregates	20-30 µm	Green-yellow, minor het. zonations. Numerous blue scheelite
				Dissiminated	80 µm	
09CQA1009A01	K-Fe (HT to LT) , brecciation	µm Si, Hm, Chl	Hem, Brecciated	Small, disseminated	30-50 µm, rare 60 µm	Bluish-Green
09CQA1009B01	K-Fe (HT to LT) , brecciation	µm Si, Hm ±Chl	Hem, Brecciated	Rare in relict clasts, often in within large hm.	60 - 80 µm, up to 100 µm	Typical Green. Blue core, Green rim

ID	Alteration	Mineral replacement	Veins	Apatite location/Association	Apatite size	CL, additional information
2507A	K-Fe (HT) alteration, brecciation	Mag, Clay.	Mag, Hem, Brecciated	Dissiminated	0.2 to >3 mm	Blue CL, green where altered. Blue concentric zonations in some crystals.
11PUA086B04	Ca-Fe (HT) alteration	-	-	Dissiminated, mantled by muscovite	0.2 to >3 mm	Blue CL, green where altered. Blue concentric zonations in some crystals.
11PUA538D01	Ca-Fe (HT), K-Fe alteration	-	-	Rare, dissiminated	300 to 400 µm	Typical Green. Blue core, Green rim
11PUA538C01	Ca-Fe (HT), K-Fe alteration	-	-	In relict mafic zones	300 to 400 µm	Grayish-blue, green edges
11PUA084C01	Ca-Fe (HT) alteration	-	-	Dissiminated	300 to 500 µm	Typical Green. Blue core, Green rim

Apatite occurrence

Four texturally distinct types of apatite occurrence were observed:

1) Apatite associated mostly with volcaniclastic samples commonly occurs in dull brownish polycrystalline aggregates of silt and clay size minerals (e.g. 09CQA0026E01). This is the most fine-grained apatite population, with crystals typically ranging between 20-40 µm in size. Apatite crystals from this population are usually free of inclusions and euhedral. The aggregates are associated with hematite staining and magnetite crystals and are often clearly visible in CL, contrasting with the faint blue background from the feldspars (e.g. 09CQA0026E01; 09CQA0011B01). This type of apatite is texturally similar to metasomatic apatite described by Rae et al. (1996) found in association with mafic Ca-rich phases, including aegirine-augite and amphibole, within a heavily metasomatised quartzite.

2) The second population of apatite occurs as single crystals often found within veinlets or patches of slightly coarser microcrystalline silica. These crystals are typically larger than the first type of apatite, ranging between 60-80 µm in size, and they usually show pitted edges, sometimes with a partial hematite coating. This type of apatite commonly contains numerous fluid-filled inclusions (09CQA0109D03), and/or monazite (09CQA0026C01) and hematite (09CQA0011B01) inclusions.

3) The third type of apatite is less common and consists of large crystals ranging between 100-300 µm in size (09CQA0109F02; 09CQA0013A01). These large crystals are mostly occurring in late epidote veins. Scheelite may be present within these same veins. Apatite from this group shows a heterogeneous zoning in CL with the response varying in intensity but not in color.

4) A fourth type of apatite was found in samples from the Sue-Dianne mineralized breccia (2507A, 09CQA1009A1, 09CQA1009B1) and from the Fab Lake IOCG system (11UPA086B04, 11UPA538D01, 11UPA538C01, 11UPA084C01). This type of apatite shows larger crystals (0.2 to 3 mm) which display a CL zoning consisting of two characteristic colors: a main blue zone that was shown by SEM-EDX to contain a higher concentration of REEs, and smaller green zones, which have lower concentrations of REEs or concentrations below detection limit (e.g. 2507A). Usually, the core of these apatite crystals consists of a blue zone; rims and areas bordering fractures are green (e.g. 2507A). This population of apatite is found in three distinct associations: 1) randomly disseminated in massive magnetite, in which case it is often surrounded by clay minerals (2507A); 2) associated with hematite aggregates and chlorite veins in heavily altered samples from Sue-Dianne (09CQA1009A1, 09CQA1009B01); and 3) randomly disseminated among the muscovite in the Fab Lake IOCG system samples.

DISCUSSION

The majority of apatite crystals identified in the studied samples show clear evidence of metasomatic alteration in the form of irregular compositional zonation patterns visible in CL. Apatite crystals occur predominantly in aggregates or in deformed, relict veinlets, indicating their early emplacement by hydrothermal fluids and subsequent alteration. Apatite is also abundant in some of the later epidote-bearing veinlets which crosscut hydrothermal minerals such as earlier apatite, clearly indicating numerous distinct episodes of apatite formation and alteration. Because of this complex history, no distinction was possible between a magmatic apatite population present in protolith later affected by hydrothermal fluids (either through overgrowth crystallization or being partially dissolved), and an original hydrothermal apatite population. A few disseminated apatite crystals were observed without any textural association with veins, aggregates or specific mineral replacements. These apatite crystals do not show any morphological or geochemical variation (based on CL and EDX work) from the apatite occurring in aggregates or in veinlets.

Apatite with a blue-green color response in CL is seen in the mineralized samples from Sue Dianne (2507A, 09CQA1009A01 and 09CQA1009B01) and in samples from the Fab Lake system (11UPA086B04, 11UPA538D01, 11UPA538C01, 11UPA084C01). Since samples from both systems show a similar green zoning of the blue apatite along fractures within the crystals and in the form of stringers, we infer that the green zones are secondary in these particular crystals and are associated with REE-depleted fluids present after crystallization in both cases. Fe-rich fluids were subsequently introduced but had little effect on the apatite other than a hematite staining present in both CL zones.

SUGGESTIONS FOR FUTURE WORK

CL optical microscopy has proven to be essential for the identification of fine grained apatite and for the characterization of crystal zoning. Given its potential and low cost, this analytical method is, in our opinion, under-utilized in the study of apatite. Alternatively, apatite could be located by automated EDX scanning for phosphorus. The diagenesis of each of the four apatite populations found in the Sue Dianne, Brooke and Fab Lake systems remains poorly understood. Specific associations between each alteration phases and the morphological characteristics of apatite stated above is currently being examined as a continuation of this study.

Only the apatite populations #3 and #4 contain grains large enough to be hand-picked under a binocular. All grains from the first population and most grains from the second population will be incorporated into the silt and clay fraction of the till during glacial attrition. A normalized count of grains with a blue CL response picked from till samples could offer potential for using apatite as an indicator mineral provided that a characterization of apatite from a larger variety of systems across the IOCG spectrum is completed. Re-examination of apatite grains separated from till and bedrock samples from across the GBmz and regrouped into the four apatite populations, as well as CL characterization prior to mounting, is being completed to better assess the validity of using apatite as an indicator mineral for exploration in the early stages of processing.

ACKNOWLEDGEMENTS

This research was conducted as part of an undergraduate thesis by P. Lypaczewski at McGill

University. Samples were collected as part of the Geomapping for Energy and Minerals (GEM) IOCG Project under the leadership of Louise Corriveau at the Geological Survey of Canada, in collaboration with the Northwest Territories Geoscience Office through funding from the Strategic Investments in Northern Economic Development Program at Indian and Northern Affairs Canada. We are grateful to the following: Fortune Minerals Ltd. for logistical support at NICO in 2009 and 2010 and Helen Campbell and John Stix for respectively making the SEM and CL analysis possible. Jean-François Montreuil is thanked for providing a careful review.

REFERENCES

Averill, S. A. 2001. The application of heavy mineral indicator mineralogy in mineral exploration, with emphasis on base metal indicators in glaciated metamorphic and plutonic terrain. In: McClenaghan, M.B. Bobrowsky, P.T. Hall, G.E.M., Cook, S.J. (eds) Drift exploration in glaciated terrain. Geological Society, London, Special Publications, vol. 185, p. 69-82.

Belousova, E.A. Griffin, W.L. O'Reilly, S.Y. Fisher, N.I. 2002. Apatite as an indicator mineral for mineral exploration: trace-element compositions and their relationship to host rock type. J. Geochem. Expl. 76, p. 45–69.

Bonyadi, Z. Davidson,G. Mehrabi, B. Meffre, S. Ghazban, Fereydoun. 2011, Significance of apatite REE depletion and monazite inclusions in the brecciated Se–Chahun iron oxide–apatite deposit, Bafq district, Iran: Insights from paragenesis and geochemistry. Chemical Geology, v. 281, p. 253-269.

Bouzari, F. Hart, C.J.R. Barker, S. & Bissig, T. 2011. Porphyry indicator minerals (PIMS): A new exploration tool for concealed deposits in south-central British-Columbia. Geoscience BC Report 2011-17.

Camier, W. J. 2002, The Sue-Dianne Fe-oxide Cu-Ag-Au breccia complex, southern Great Bear Magmatic Zone, Northwest Territories, Canada: Unpublished M.Sc. Thesis, University of Western Ontario, London, Ontario, 210 p.

Coulson, I.M. & Chambers, A.D. 1996. Patterns of zonation in rare-earth-bearing minerals in nepheline syenites of the North QoroQ center, South Greenland. Canadian Mineralogist v. 34, p. 1163-1178

Corriveau, L. Williams, P.J. Mumin, A.H. 2010. Alteration vectors to IOCG mineralization: From uncharted terranes to deposits. In Corriveau, L. and Mumin, A.H. eds. Exploring for iron oxide copper-gold deposits: Canada and global analogues; Geological Association of Canada, Short Course Notes 20, p. 89-110

Gandhi, S.S. Mortensen J.K. Prasad, N. Van Breemen, O. 2001. Magmatic evolution of the southern Great Bear continental arc, northwestern Canadian Shield: geochronological constraints. Canadian Journal of Earth Sciences, v. 38, p. 767-785.

Harlov, D.E. Wirth, R. Förster, H.-J. 2005. An experimental study of dissolution-reprecipitation in fluorapatite: Fluid infiltration and the formation of monazite. Contributions to Mineralogy and Petrology, v. 150, p. 268–286.

Harlov, D.E. and Förster, H.-J. 2003. Fluid-induced nucleation of REE-phosphate minerals in apatite: Nature and experiment. Part II. Fluorapatite. American Mineralogist, v. 88, p. 1209–1229.

Harlov, D.E. Förster, H.-J. Nijland, T.G. 2002a. Fluid-induced nucleation of REE-phosphate minerals in apatite: Nature and experiment. Part I. Chlorapatite. American Mineralogist, v. 87, p. 245–261.

Harlov, D.E. Andersson, U.B. Förster, H.-J. Nyström, J.O. Dulski, P. Broman, C. 2002b, Apatite-monazite relations in the Kiirunavaara magnetite-apatite ore, northern Sweden. Chemical Geology, v. 191, p. 47–72.

Kempe, U. and Götze, J. 2002, Cathodoluminescence (CL) behaviour and crystal chemistry of apatite from rare-metal deposits: Mineralogical Magazine, v. 66, p. 151–172.

Mumin, A.H. Somarin, A.K. Jones, B. Corriveau, L. Ootes, L. Camier, J. 2010. The IOCG-porphyry-epithermal continuum of deposits types in the Great Bear Magmatic Zone, Northwest Territories, Canada. In Corriveau, L. and Mumin, A.H. eds. Exploring for iron oxide copper-gold deposits: Canada and global analogues; Geological Association of Canada, Short Course Notes 20, p. 59-78.

Murray, J.R. and Oreskes, N. 1997. Uses and limitations of cathodoluminescence in the study of apatite paragenesis. Economic Geology, v. 92, p. 368-376

Normandeau, P.X. McMartin, I. Paquette, J. Corriveau, L. 2011. Drift prospecting applied to iron oxide copper gold exploration in the Great Bear magmatic zone, Northwest Territories, Canada. Poster presentation, Geological & Mineralogical Association of Canada (GAC-MAC) annual meeting 2011, 25-27 April, Ottawa.

Potter, E.G. Montreuil, J.-F. Corriveau, L. 2012. Alteration mapping in IOCG systems: Fab Lake case study. Geological Association of Canada – Mineralogical Association of Canada Annual Meeting, Program with Abstracts, v. 35, p. 110.

Rae, D.A. Coulson, I.M. & Chambers, A.D. 1996. Metasomatism in the North Qoroq centre, South Greenland: Apatite chemistry and rare-earth element transport. Mineral. Mag. v.60, p. 207 -220.

Slave geological province NATMAP project in Northwest Territories, Canada. GSC Open File 2559. Last DIF reviewed: 2006.

De Toledo, M.C.M. Lenharo, S.L.R. Ferrari, V.C. Fontan, F. DeParseval, P. 2004. The compositional evolution of apatite in the weathering profile of the Catalão 1 alkaline-carbonatitic complex, Goias, Brazil, The Canadian Mineralogist, v. 42, p. 1139-1158.